



# Biological Alteration of Flow Properties of Soil Samples From Two Bt Horizons of a Haplic Luvisol Determined With Rheometry

Christoph Haas<sup>1,2\*</sup>, Dörthe Holthusen<sup>3</sup> and Rainer Horn<sup>1</sup>

<sup>1</sup> Institute for Plant Nutrition and Soil Science, CAU Kiel, Kiel, Germany, <sup>2</sup> Institute of Soil Landscape Research, Leibniz Centre for Agricultural Landscape Research, Müncheberg, Germany, <sup>3</sup> Department of Soil Science, Federal University of Santa Maria, Santa Maria, Brazil

## OPEN ACCESS

### Edited by:

Andrea Carminati,  
University of Bayreuth, Germany

### Reviewed by:

Thomas Keller,  
Swedish University of Agricultural  
Sciences, Sweden  
Muhammad Naveed,  
University of the West of Scotland,  
United Kingdom

### \*Correspondence:

Christoph Haas  
c.haas@soils.uni-kiel.de

### Specialty section:

This article was submitted to  
Soil Processes,  
a section of the journal  
Frontiers in Environmental Science

**Received:** 14 March 2018

**Accepted:** 07 September 2018

**Published:** 02 October 2018

### Citation:

Haas C, Holthusen D and Horn R  
(2018) Biological Alteration of Flow  
Properties of Soil Samples From Two  
Bt Horizons of a Haplic Luvisol  
Determined With Rheometry.  
*Front. Environ. Sci.* 6:110.  
doi: 10.3389/fenvs.2018.00110

Flow properties of soils are helpful to describe the soils' response on mechanical loading, which occurs naturally (e.g., caused by growing roots or drilling earthworms) or anthropenically (e.g., in the course of management practices like tillage) In order to determine the effect of bacterial or plant exudation induced changes of soil strength and soil's flow behavior soil samples of the Bt horizons of a haplic Luvisol were saturated with pure water or with aqueous solutions of biological model substance. We chose xanthan gum as a bacterial exudate which represents the chemical alteration of soil microorganism, while polygalacturonic acid has been used as a root's mucilage analog. Surface tension and viscosity of these aqueous solutions were determined, and soil samples' flow properties were obtained with the help of rheometry. By applying amplitude sweep tests to the soil samples soil stability related parameters were determined [loss ( $G''$ ) and storage ( $G'$ ) moduli, representing the plasticity or elasticity of soils, respectively] or calculated [namely, the loss factor (ratio of  $G'''$  and  $G'$ ), Integral Z (a strain-stress dependent sum-parameter) and the linear viscoelastic range (where no changes in soil structure occur)]. We hypothesized that (I) flow properties of used model substances differ from those of pure water and, (II) biological model substances influence the water content at defined matric potential caused by e.g., altered surface tension, thus influencing parameters that were related to soil stability. Furthermore, (III) the impact of biological model substance depends on the shear rate that is applied to achieve the soil's deformation because some biological model substances show non-Newtonian flow. So far and to our knowledge this is the first rheological work on soils that evaluates the effect of differing shear rates on elastic and plastic deformation statistically. We found the impacts of biological model substances on soils' flow properties to be not only dependent of origin (plant or bacterial), concentration and matric potential, but also on deformation intensities. Due to chemical particularities of PGA a deformation induced soil stabilization was observed. Leading to the conclusion that deformation processes e.g., in the rhizosphere are much more complex than previously thought.

**Keywords:** amplitude sweep test, polygalacturonic acid, xanthan, rheology, viscosity, surface tension

## INTRODUCTION

Biological processes like plant roots' or soil microorganisms' exudation result in chemically and physically alterations of soil properties. For example, plant roots' mucilage exudation (Tisdall and Oades, 1979) or biological reallocation or transformation (e.g., caused by earthworms or microorganisms, Hoang et al., 2016; Banfield et al., 2017) of organic compounds results in changes in chemical parameters [e.g.,  $\text{CaCO}_3$  production, SOC accumulation (Jones et al., 2009), changes in pH and redox (Uteau et al., 2015) or in altered ion concentrations (Carvalhais et al., 2011)], and coincides with altered physical properties, like aggregation (Six et al., 2004). These physical alterations result in,

- (I) decreased soil stability, for example, caused by microorganisms that oxidize gluing compounds (like particulate organic matter, Six et al., 2004) or neutralize cementing agents (like  $\text{CaCO}_3$ ) by  $\text{H}^+$  release or by applying shear stresses to the soil at moist conditions, for example caused by a growing root.
- (II) increased stabilities directly caused by the exudation, likegluing effects or an increased surface tension of the soil solution and therewith indirect effects on wetting properties which diminishes the disrupting impact of swelling (Hallett and Young, 1999; Chenu et al., 2000) Two exemplary substances for cementing and gluing are Xanthan gum and polygalacturonic acid. The former is an anionic polysaccharide that is often used as a food additive (Zhang et al., 2008). It is produced by fermentation or by exudation of *Xanthomonas campestris* bacterium. The basic chemical structure of Xanthan gum ( $\text{C}_{35}\text{H}_{49}\text{O}_{29}$ ) is a linear linked  $\beta$ -D glucose backbone with a trisaccharide side chain on every other glucose. A well-known characteristic is its pseudo-plasticity (i.e., shear thinning). Acid sugars are found on root surfaces and on cells walls. They occur as monomers or polymers. One polymer, for example, is polygalacturonic acid (PGA), which occurs as chains and is the main constituents of root mucilage (Manunza et al., 1997). For example, PGA-chains linked by  $\text{Ca}^{2+}$  act as model of the soil root interface, because it exhibits a fibrillary structure similar to that of natural mucilage (Manunza et al., 1997). Both substances form gels, having the potential to alter the pore-size distribution in soils. Furthermore, since both substances are negatively charged at most soil conditions (not too acidic soil) they are bond to negative charged clay particles by polyvalent cations like  $\text{Ca}^{2+}$  and  $\text{Mg}^{2+}$ .

Soil stability defines not only the trafficability of soils (Riggert et al., 2017) but also plant root growth processes (Bengough and Mullins, 1990). As shown by Markgraf et al. (2006), rheometry delivers a set of parameters that are related to microstructural soil stability of which the most important are (Figure 1): The shear stress, which is required for soil deformation and which represents the capability of the soil to withstand the deformation. The storage modulus,  $G'$ , which is a measure for the elasticity of a soil. It represents the energy that is available to reverse the gradual increase of soil distortion, while the loss modulus  $G''$  equals the

dissipated energy (Mezger, 2014). The deformation where  $G'$  equals  $G''$  is called cross-over. With deformations larger than the cross-over the viscous behavior of the samples overweighs the elastic component. The samples' structural integrity is irreversibly destroyed which may result in creeping or flowing, depending on the water content of the sample (Markgraf and Horn, 2006; Holthusen et al., 2010; Mezger, 2014). Markgraf et al., 2012 introduced a semi-quantitative parameter which is calculated according to Equation (1) and named Integral  $z$ , abbreviated to  $I_z$  in this manuscript.

$$I_z = \int_{0.001}^{\text{cross-over}} (1 - G''G'^{-1}) dy \quad (1)$$

Since  $I_z$  is integrated over the deformation, the flow behavior at small deformations is mostly neglected but influenced by larger strains which leading to higher similarity of values for  $I_z$  (Holthusen et al., 2017). The linear viscoelastic (LVE) region, and  $I_z$  are derived parameters from  $G'$  and  $G''$ . Within the LVE region there are no significant changes in the structure of the sample. Soil stability is linked to hydraulic capacities like the pore-size distribution or the water content (Riggert et al., 2017) and to intensities like (un-)saturated hydraulic conductivity (Fazekas and Horn, 2005; Riggert et al., 2017).

Alterations of flow properties (e.g., viscosity and surface tension) of the soil solution potentially result in altered hydraulic capacities and intensities (Holthusen et al., 2012) influencing not only the soil strength but the plant-roots' water uptake, and consequently, the productivity of agriculturally used soils. For example, the surface tension influences the amount of plant-available water, and, due to adhesive forces also the soil stability. The viscosity influences intensities like the (un-) saturated hydraulic conductivity: The flow of water is described by Darcy's law. The volume of water that flows in a defined time through a given area decreases linearly with increasing viscosity, and vice versa. An increased viscosity results in decreased plant water uptake per unit of time.

The aim of this study was to quantify biological alterations of flow properties and of parameters related to microstructural soil stability as derived from amplitude sweep tests.

We hypothesized that (I) flow properties of used model substances differ from those of pure water and, (II) biological model substances influence the water content at defined matric potentials caused by altered flow properties, and with that, parameters related to soil stability as derived from amplitude sweep tests. Furthermore, (III) the impact of biological model substance depends on the shear rate that is applied to achieve the soils' deformation because some biological model substances show non-Newtonian flow. So far and to our knowledge this is the first rheological work on soils that evaluates the effect of differing shear rates on elastic and plastic deformation (represented as loss factor) statistically.

## MATERIALS AND METHODS

### Soil Material

Disturbed soil material was excavated in September 2014 from two layers (Bt-1 from 0.45 to 0.55 m, and Bt-2 from 0.55 to

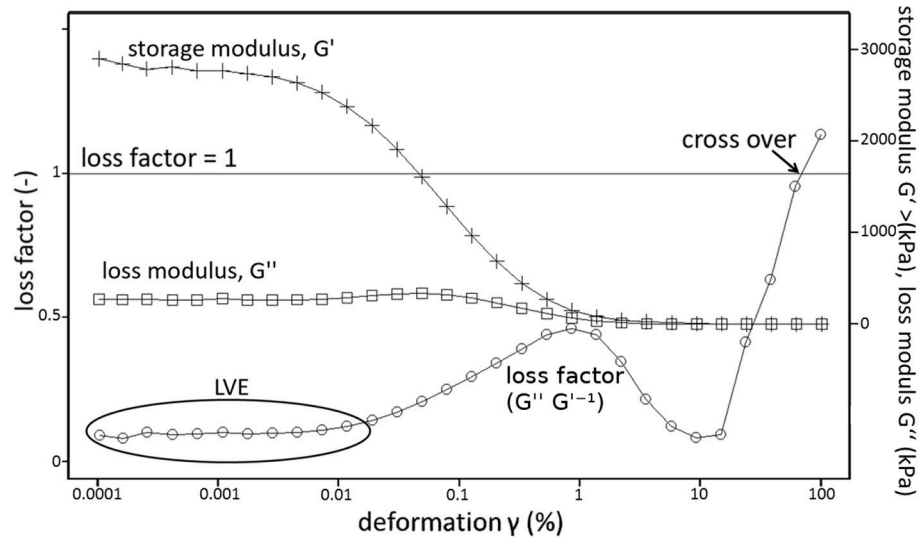


**FIGURE 1** | Exemplary curves for linear viscoelastic range (LVE), storage modulus ( $G'$ ), loss modulus ( $G''$ ), and their ratio (loss factor,  $G''/G'$ ) as well as the cross over.

**TABLE 1** | Sand, silt, clay, as well as, soil organic carbon (SOC) contents in  $\text{g kg}^{-1}$  soil, as well as, pH, and electrical conductivity (eC) in  $\mu\text{S cm}^{-1}$  of the four pits where soil cores were excavated from a loess-derived Luvisol, Klein-Altendorf near Bonn, Germany.

Pit	Depth m	Sand	Silt Clay		SOC	pH	eC $\mu\text{S cm}^{-1}$
			$\text{g kg}^{-1}$				
24	0.45–0.55	71.4	780	149	4.0	7.0	83
24	0.55–0.65	66.1	730	204	5.8	7.03	74
40	0.45–0.55	54.7	650	295	4.5	6.99	100
40	0.55–0.65	44.8	710	245	3.4	7.11	83
57	0.45–0.55	59.8	770	170	3.9	7.02	81
57	0.55–0.65	44.6	740	215	4.1	7.0	71
74	0.45–0.55	58.9	660	281	4.0	6.98	104
74	0.55–0.65	40.0	700	260	3.8	7.02	77

0.65 m) of a Bt horizon from a haplic Luvisol (IUSS Working Group WRB, 2006) in four repetitions (i.e., from four pits) of a totally randomized trial (Kautz et al., 2014) at the experimental area of Campus Klein-Altendorf ( $50^{\circ}37'9''$  N  $6^{\circ}59'29''$  E, University of Bonn, Germany). The site is characterized by a maritime climate with temperate humid conditions ( $9.6^{\circ}\text{C}$  mean annual temperature, 625 mm annual rainfall). Main soil properties are listed in **Table 1**. The Bt horizon is characterized by accumulated clay, leached from the A-horizon (0–0.27 m) and the E horizon (0.27–0.41 m). Chicory (*Cichorium intybus* L. “Puna,”  $5 \text{ kg ha}^{-1}$  seeding rate) had been grown in these trials for the last three years. With its herringbone or monopodial branching root systems *Cichorium intybus* L. penetrates deep into the subsoil exploring for water and nutrient supply (Kautz et al., 2012).

## Determination of Flow Properties of Aqueous Solutions of Biological Model Substances

Dynamic viscosity of aqueous solutions of biological model substances and of water were determined with a rheometer (MCR300, Anton Paar, Stuttgart, Germany) and a standardized cone-plate measuring system ( $0.5^{\circ}$  cone angle, gap size =  $50 \mu\text{m}$ ) with a shear rate ramp ranging from 10 to  $1,000 \text{ s}^{-1}$ . Within this shear rate ramp 29 sampling points were considered. Viscosity was calculated using the rheometers’ software RheoPlus (Anton Paar, Stuttgart, Germany). The samples’ volume was  $400 \mu\text{l}$ . Surface tensions were determined with the help of a microtensiometer (Krüssensometer, Krüss, Hamburg, Germany) and the Wilhelmy-plate method (with a platinum plate) as described by Mohamed et al. (2010). The sample volume was 50 ml. The platinum plate was inserted (2 mm) into the fluid. Ten sampling points were considered while the plate was pulled out of the fluid. The test duration was 60 s. All measurements were performed at laboratory conditions ( $T = 293.15 \text{ K}$ ) with  $n = 5$ . The temperature was checked using a thermometer.

## Biological Model Substances and Sample Preparation for Amplitude Sweep Test

Soil was sieved to  $\leq 2 \text{ mm}$  and refilled to small cylinders, 0.9 cm in height, and 3.6 cm in diameter ( $V = 9.2 \text{ cm}^3$ ). Aqueous solutions of two biological model substances were used to saturate the samples and to determine biological alterations of biopore walls: (I) Polygalacturonic acid [abbreviated PGA;  $(\text{C}_6\text{H}_8\text{O}_6)_n$ ,  $\sim 95\%$  (enzym.), Fluka BioChemika 81325, EC No. 2116826, Gillingham, United Kingdom] which was identified as a model root exudate (Morel et al., 1987; Gessa and Deiana, 1992; Gessa et al., 1997; Czarnes et al., 2000; Traoré et al., 2000; Grimal et al., 2001; Zhang et al., 2008). PGA was solubilized by adding

0.51 ml of 1 M KOH for 100 mg PGA and diluted with double-distilled water. (II) Xanthan gum from *Xanthomonas campestris* (Sigma-Aldrich, G1253, EC No. 234-394-2) was mixed with double-distilled water using a magnetic stirrer. Three defined concentrations from model substances were tested, namely, 1, 2, and 3 gL<sup>-1</sup>. Three samples per pit, depths, model substance, as well as concentration and five control samples (0 gL<sup>-1</sup>) were saturated by capillary rise. Measurements were performed at four matric potentials [namely,  $\Psi_m = -1, -3, \text{ and } -6$  kPa (drained with the help of sand beds) or  $-30$  kPa (drained on ceramic suction plates)].

## Amplitude Sweep Test (AST) and Volumetric Water Contents

A profiled parallel plate measurement system, 0.025 m in diameter, was used to perform the AST with a rheometer MCR300 (Anton Paar, Stuttgart, Germany). The soil samples (9 mm in height) were cut in halves horizontally. The lower half of the sample was placed on the lower plate of the rheometer. The upper half of the sample was used to determine volumetric water contents (= before measurement). The lower plate is fixed while the upper one is moving in an oscillating manner with

successively increasing amplitudes at a constant frequency of 0.5 Hz. Controlled shear deformation ranged from 10<sup>-4</sup> to 100% related to the measuring gap (4 mm). More detailed information can be obtained from Markgraf et al. (2006). The remaining soil was recovered from the lower plate in order to determine the volumetric water content (= after measurement). The storage modulus ( $G'$ ), the loss modulus ( $G''$ ), and the linear viscoelastic range (LVE) were calculated using the rheometers' software RheoPlus (Anton Paar, Stuttgart, Germany), while cross-over and Integral Z were calculated manually from raw data.

## Statistical Analyses

The statistical software R (R Development Core Team, 2017) was used to evaluate the data. (I) The data evaluation started with the definition of an appropriate statistical mixed model (Laird and Ware, 1982; Verbeke and Molenberghs, 2000), including the sampling depths (qualitative: 0.45–0.55 m; 0.55–0.65 m), the concentrations of aqueous solutions [0 gL<sup>-1</sup> (for water), 1, 2, and 3 gL<sup>-1</sup>], the matric potentials (quantitative:  $\Psi_m = -1, -3, -6, \text{ or } -30$  kPa) and corresponding interaction effects, also with the biological model substances (polygalacturonic acid, Xanthan gum), as fixed factors. The investigated pits and further nested

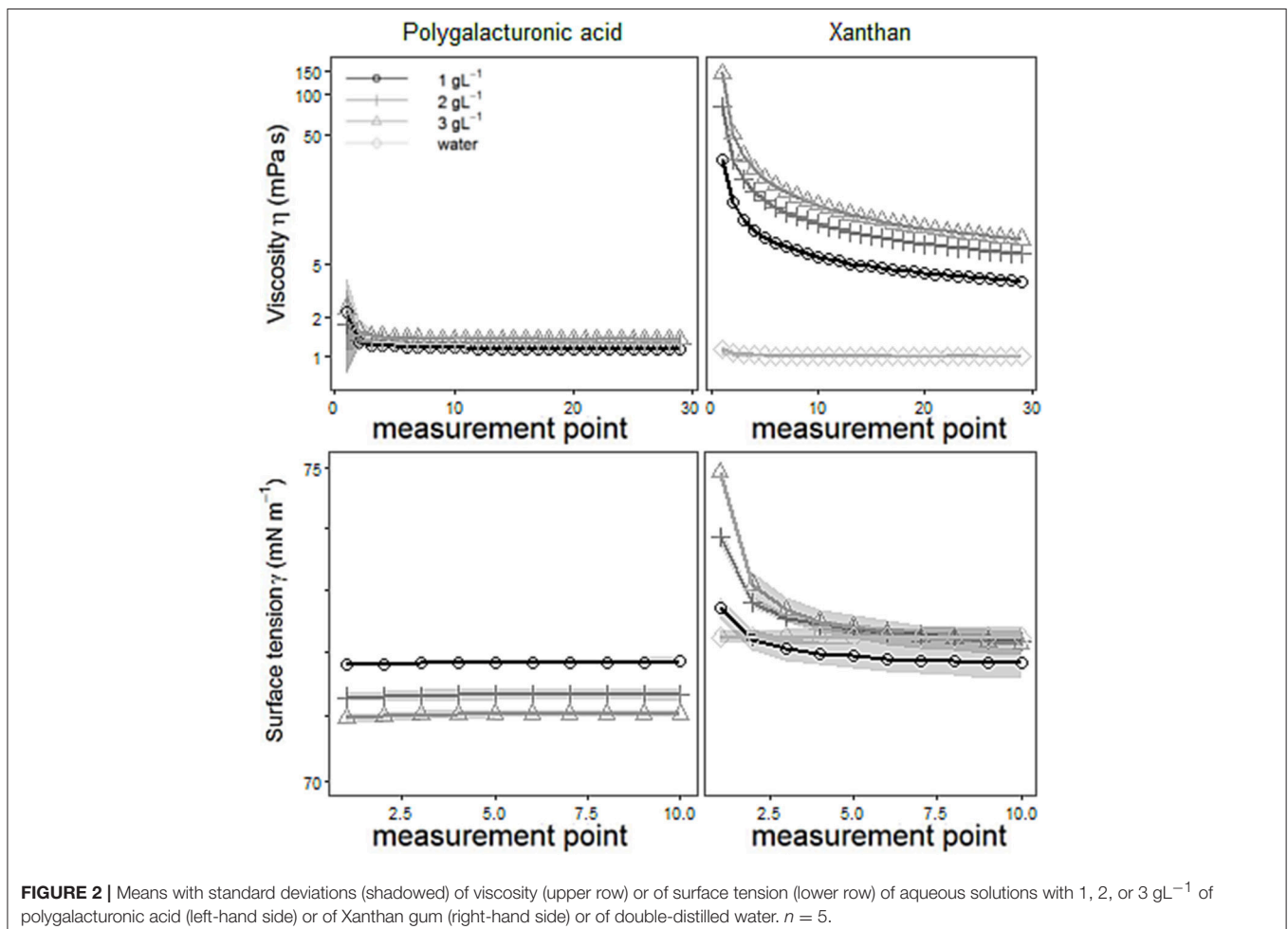
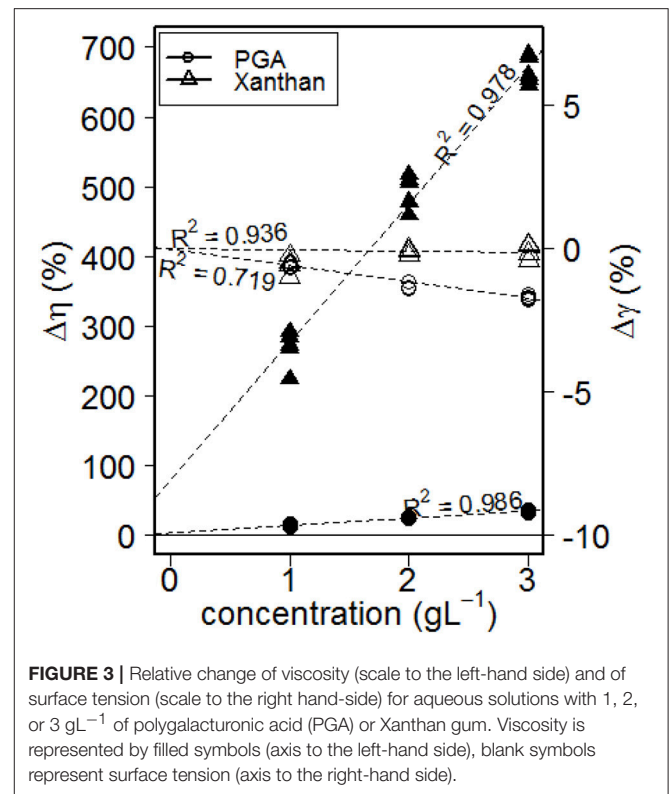


**FIGURE 2** | Means with standard deviations (shadowed) of viscosity (upper row) or of surface tension (lower row) of aqueous solutions with 1, 2, or 3 gL<sup>-1</sup> of polygalacturonic acid (left-hand side) or of Xanthan gum (right-hand side) or of double-distilled water.  $n = 5$ .

effects were regarded as random factors. The data were assumed to be normally distributed and to be heteroscedastic due to the different levels of the matric potential. These assumptions are based on a graphical residual analysis. Based on this initial model, a model selection (forward selection) based on AIC values (Akaike, 1973; Sakamoto et al., 1986) was conducted to decide which covariates can be used for prediction. After that, covariates with a variance inflation factor (VIF) of 10 or higher were removed stepwise. Finally, non-significant covariates were omitted, based on an analysis of covariances (Cochran, 1957). For the final model, a Pseudo  $R^2$  was calculated (Nakagawa and Schielzeth, 2013). The used covariates were soil organic carbon content, electrical conductivity, pH and the texture (sand, silt or clay content). (II) Single point evaluation: Here, the measurement points (1–30) were added to the statistical model to evaluate the impact of differing shear rates (named as single point evaluation, abbreviated as SPE in this manuscript). The normal force was added, additionally, beside those covariates already used for (I).

## RESULTS AND DISCUSSION

Dynamic viscosity ( $\eta$ ) for shear rates ranging from 10 to 1,000  $\text{s}^{-1}$ , and surface tensions ( $\gamma$ ) of aqueous solutions of biological model substances, and double-distilled water are shown in **Figure 2**. The addition of polygalacturonic acid (PGA) or Xanthan gum (Xanthan) increased the viscosity of double-distilled water. The more PGA or Xanthan had been added the more pronounced the change in viscosity. Considering shear rates  $\geq 187 \text{ s}^{-1}$  (=equals measurement point 6) Newtonian flow was found for PGA and double-distilled water (indicated by a constant viscosity over the applied shear rates). However, increased viscosities were found for both fluids for very small shear rates. This contradicts the fact, that pure water is a Newtonian fluid, while Stoddart et al. (1969) found PGA to be shear thinned even for larger shear rates. Thus, we have to take into account that flow behavior of water is caused by impurities of the double distilled water. For Xanthan an intense shear thinning was found, which is characterized by an under proportional increase of shear stress that is required for fluid deformation with increasing shear rates. These findings are in agreement with those described by Pettitt et al. (1995). Small amounts of Xanthan increased the viscosity disproportionately as indicated by the intercept of the regression line shown in **Figure 3**, presenting the relative change of both, viscosity and surface tension caused by the addition of PGA or Xanthan (=concentration effect). Here, values for viscosity are gathered for maximum shear rates ( $=1,000 \text{ s}^{-1}$ ), whereas those of the surface tension were obtained from the last measurement point. The change in viscosity is much more pronounced than the change in surface tension. The change in viscosity is much more pronounced for Xanthan (up to  $\sim 700\%$ , blank symbols) compared to PGA (filled symbols). The surface tension of aqueous solutions of PGA decreased with increasing concentration and showed smaller values than those for pure water. The surface tension of Xanthan remained (more or less) unchanged for 2 or 3  $\text{gL}^{-1}$  but the addition of



1  $\text{g PGA L}^{-1}$  decreased surface tension. These changes seem to follow linear trends, as indicated by high values of  $R^2$ . Read and Gregory (1997) determined the surface tension and the viscosity of mucilage gathered from *Zea mays* L. They found non-Newtonian flow behavior and a viscosity of 2.1  $\text{mPa s}$  (diluted in 70 % w/w  $\text{H}_2\text{O}$ , measured at  $20^\circ\text{C}$ ). This is confirmed by measurements presented in this study. With a view to surface tension results of this study contradict Read and Gregory (1997) who found heavily decreased values ( $<48 \text{ mN m}^{-1}$ ). PGA and mucilage differ not only in flow properties. Mucilage contains protein (Morel et al., 1986) and several different types of e.g., sugars (Morel et al., 1986; Read and Gregory, 1997) while pure PGA is protein-free and contains only one type of (an acidic) sugar (galacturonic acid). Thus we have to come to a critical statement about PGA as mucilage analog: PGA and mucilage differ in chemical and physical parameters.

The influence of drainage to defined matric potentials (namely,  $\Psi_m = -1, -3, -6, \text{ or } -30 \text{ kPa}$ ) on water content of soil saturated with water or saturated with aqueous solutions of polygalacturonic acid (PGA) or Xanthan gum (Xanthan) is shown in **Figure 4**. Means of water contents of soil samples saturated with water or with aqueous solutions of 1  $\text{gL}^{-1}$  PGA showed similar values for  $\Psi_m = -1 \text{ kPa}$  and  $-30 \text{ kPa}$ , but increased means in water content for  $\Psi_m = -3$  and  $-6 \text{ kPa}$ , indicating (I) the impact of altered flow properties of the soil solution (the viscosity of used biological model substances exceeds that of pure water), or (II) alterations of the pore size

distribution. The latter one might have had several causes: (a) soil loosening (due to decreased surface tension, resulting in lowered menisci forces) and therewith changes in aggregation, (b) the physical blockage of pores (Hallett et al., 2003), (c) gelation of biological model substance (and the coinciding formation of a secondary pore system) or (d) electrostatic interactions of anionic model substances and the soil matrix (caused by  $\text{Ca}^{2+}$  “bridge” formation or hydrogen bonding; Chang et al., 2015). The statistical evaluation supports the theory of an alternated pore system, because no significant differences between PGA and Xan were found for the volumetric water content before rheometry (Table 2,  $\theta_{\text{before}}$ ), which would be expected if the fluids viscosity would be of importance.

After rheometry, the water content depended on the fluid- (Table 2,  $\theta_{\text{PGA}}$  and  $\theta_{\text{XAN}}$ ). Differences in water contents are

more distinct for sample where positive water pressures were more pronounced and are caused by differing amounts of water that were squeezed out of pores which could be explained by differences in soil pore elasticity or by increased viscosities for Xanthan. The decrease in (recovered) volumetric water content for PGA exceeds that one of Xan by a factor of  $\sim 2.6$  ( $-0.37/-0.14$ ) with increasing concentration. Differences in regression coefficients for the concentration further support the theory of changes in the pore system because less water was recovered with increasing concentration which is in contradiction to the effect caused by viscosity (which increased with increasing concentration). Although the concentration of the fluid is of less importance for Xan compared with PGA (Table 2,  $\theta_{\text{PGA}}$  and  $\theta_{\text{XAN}}$ , coefficient c) more water can be recovered from samples of Xan. Due to altered water

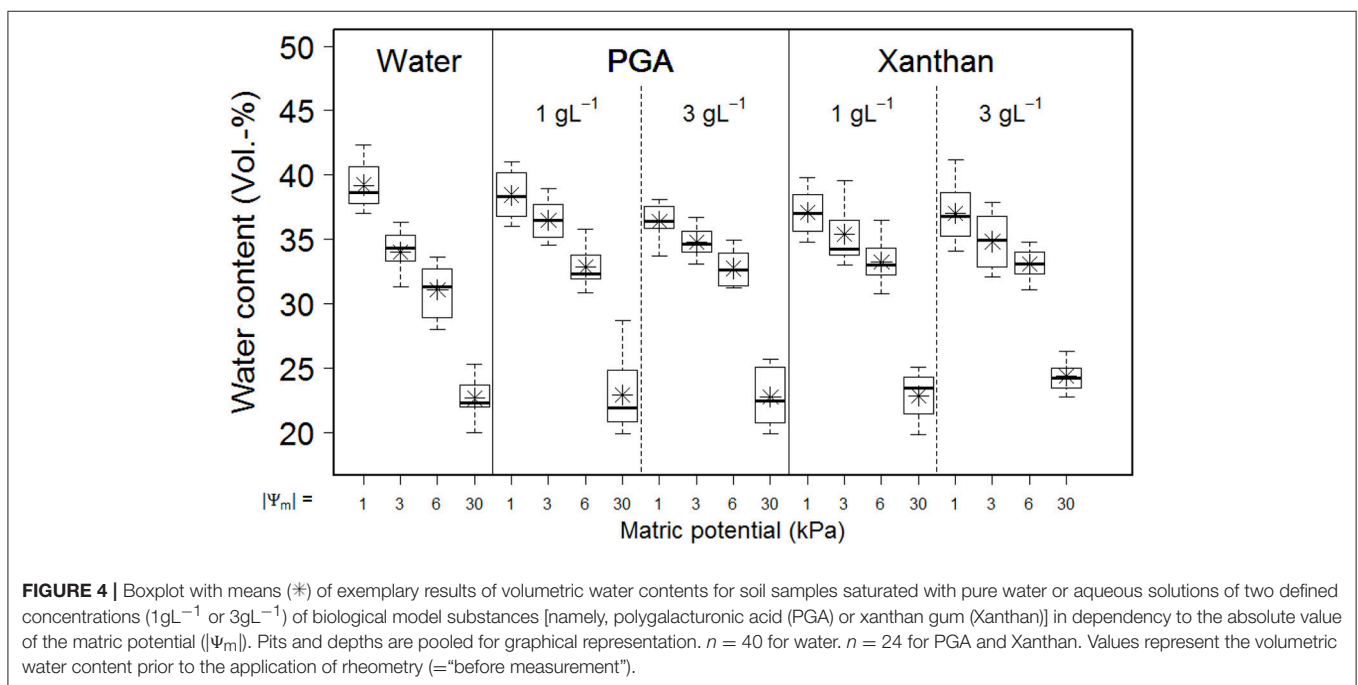


**FIGURE 4 |** Boxplot with means (\*) of exemplary results of volumetric water contents for soil samples saturated with pure water or aqueous solutions of two defined concentrations ( $1\text{ gL}^{-1}$  or  $3\text{ gL}^{-1}$ ) of biological model substances [namely, polygalacturonic acid (PGA) or xanthan gum (Xanthan)] in dependency to the absolute value of the matric potential ( $|\Psi_m|$ ). Pits and depths are pooled for graphical representation.  $n = 40$  for water.  $n = 24$  for PGA and Xanthan. Values represent the volumetric water content prior to the application of rheometry (=“before measurement”).

**TABLE 2 |** Regression coefficients (with standard error in brackets) and  $p$ -value for selected rheological parameters as derived from analysis of covariance.

parameter	coefficient			p-value		
	a	b	c	a	b	c
$\theta_{\text{before}}$ (vol.-%)	38.78 (0.78)	0.48 (0.01)	-0.64 (0.01)	<0.0001	<0.0001	<0.0001
$\theta_{\text{PGA}}$ (vol.-%)	37.04 (0.72)	0.46 (0.01)	-0.37 (0.11)	<0.0001	<0.0001	<0.0001
$\theta_{\text{Xan}}$ (vol.-%)	37.04 (0.72)	0.46 (0.01)	-0.14 (0.11)	<0.0001	<0.0001	0.22
$\text{LVE}_{\text{PGA}}$ (%)	0.008 (0.0006)	$4.5 \cdot 10^{-5}$ ( $2.0 \cdot 10^{-6}$ )	$4.0 \cdot 10^{-4}$ ( $22.3 \cdot 10^{-5}$ )	<0.001	0.023	0.083
$\text{LVE}_{\text{Xan}}$ (%)	0.008 (0.0006)	$4.5 \cdot 10^{-5}$ ( $2.0 \cdot 10^{-6}$ )	$-11.8 \cdot 10^{-4}$ ( $22.3 \cdot 10^{-5}$ )	<0.001	0.023	<0.0001
$\text{LVE}_{\text{PGA}}$ (Pa)	27.82 (11.81)	-14.49 (1.4)	14.23 (4.9)	0.128	<0.0001	0.005
$\text{LVE}_{\text{Xan}}$ (Pa)	27.82 (11.81)	-5.98 (1.7)	-11.14 (5.3)	0.128	0.0004	0.041
$l_z$	7.15 (0.55)	-1.04 (0.05)	-1.20 (0.23)	0.001	<0.0001	<0.0001
Cross over <sub>PGA</sub>	21.4 (1.15)	-1.59 (0.11)	-2.85 (0.55)	<0.001	<0.0001	<0.0001
Cross over <sub>Xan</sub>	21.4 (1.15)	-0.53 (0.11)	-0.71 (0.59)	<0.001	<0.0001	0.23

Coefficient a represents the y-intercept, b the influence of the matric potential ( $\Psi_m$ ), and the concentration effect ( $\text{gL}^{-1}$  PGA or Xan).

contents we would expect a higher soil rigidity for Xan samples, caused by a more rarely occurrence of positive pore water pressures, which lead to a larger amount of recovered water. This was found for cross over values (Table 2) but not for LVE or  $I_z$ .

The linear viscoelastic region (LVE, soil samples remain stable) can be described with maximal values for the deformation Figure 6, Table 2,  $LVE_{PGA}$  (%) and  $LVE_{Xan}$  (%) and the corresponding shear stress [Table 2,  $LVE_{PGA}$  (Pa) and  $LVE_{Xan}$  (Pa)].

The statistical analysis showed in both cases significant influences of the matric potential [=increase with a more negative matric potential, fluid independent for LVE (%) or fluid dependent for LVE (Pa)] and of the concentration (fluid dependent). LVE increases with increasing concentrations of PGA but decreases with increasing concentrations of Xan. This contradicts Hallett et al. (2003) who assumed soil loosening with PGA at low deformation ranges. However, further statistical analyses enabled a more detailed evaluation of the results, and are shown in the second part of Results and Discussion. Different

regression coefficients for matric potential [LVE (Pa)] prove a much more pronounced soil stabilizing effect with increasing drainage for PGA compared to Xan.

The soil samples structural failure can be described with  $I_z$  or with crossover (%) (Table 2).

The statistical analysis showed an effect of the matric potential and a fluid independent ( $I_z$ ) or fluid dependent [crossover (%)] effect for the concentration. Both parameters increase with progressing drainage, indicating an increased soil stability, or decrease with increasing concentrations of the model substances (Figure 6). For crossover, both effects are less pronounced for Xanthan than for PGA, indicating reduced soil rigidity for samples saturated with Xan. The less intense effect for matric potential (3-fold = 1.59/0.53) of Xan is possibly caused by an altered pore size distribution (wetter with more negative matric potentials), while the 4-fold (2.85/0.71) higher concentration effect of PGA is caused by more pronounced soil loosening effects of PGA. This proves an effect of PGA contradicting to Hallett et al. (2003) (= a soil loosening effect for increased concentrations of PGA at higher deformations/shear rates).

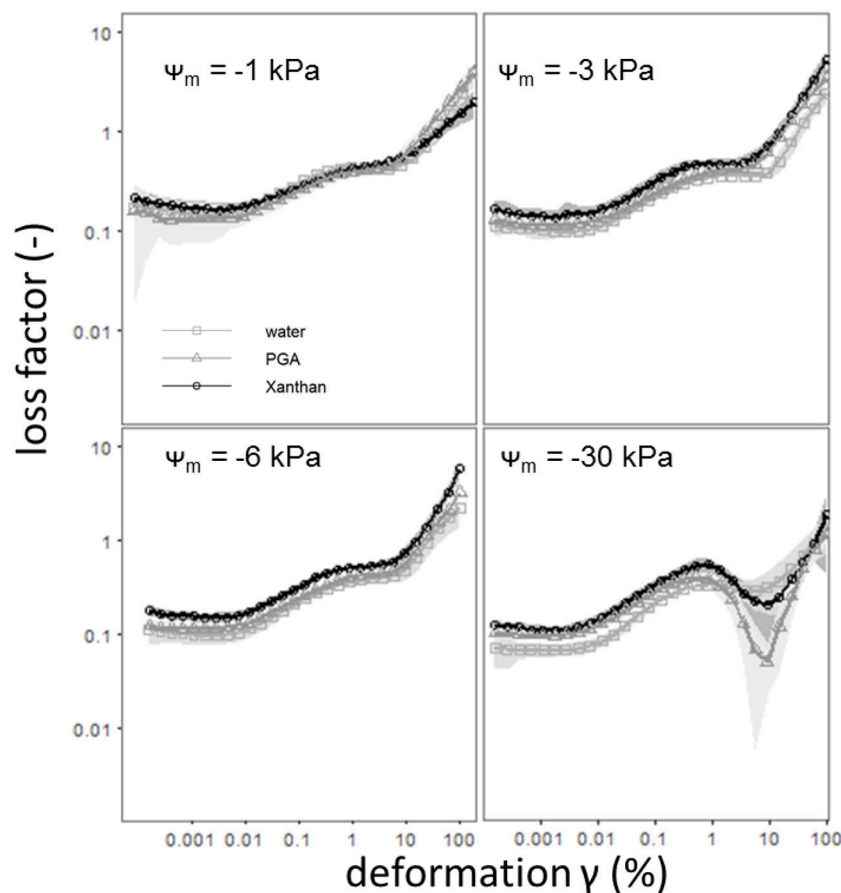


**FIGURE 5** | Means with standard deviations (shaded) of the loss factor [defined as the ratio of loss ( $G''$ ) and storage modulus ( $G'$ )] as derived from amplitude shear tests for the complete deformation range (0.001–100 %) for soil saturated with pure water ( $\square$ ) or for soil saturated with aqueous solutions of polygalacturonic acid ( $3 \text{ gL}^{-1}$  PGA,  $\triangle$ ) or of Xanthan gum ( $3 \text{ gL}^{-1}$  Xanthan,  $\ominus$ ) for defined matric potentials, namely  $\Psi_m = -1 \text{ kPa}$ ,  $-3 \text{ kPa}$ ,  $-6 \text{ kPa}$  or  $-30 \text{ kPa}$ . Pits and depths are pooled for graphical representation.  $n = 40$  for water.  $n = 24$  for PGA and Xanthan.

However, since the parameters ( $I_z$ ) are sensitive for larger shear rates (Holthusen et al., 2017) we need to take into account that flow behavior is deformation dependent, which has been shown in several studies, but has never been evaluated statistically. **Figure 5** shows differing flow behavior for soils mixed with various biological model substances and for differing deformations. Means with standard deviations of the loss factor as derived from amplitude sweep tests for the complete deformation range (0.001–100 %) for soil mixed with water and for soil mixed with 3 gL<sup>-1</sup> of polygalacturonic acid (PGA, circles or) or 3 gL<sup>-1</sup> of Xanthan for  $\Psi_m = -1, -3, -6,$  or  $-30$  kPa are shown in **Figure 5**. Here, general trends can be observed: At very low deformation intensities (0.001%) the loss factor decreases with increasing drainage (more negative matric potential), independently from the used fluid (water, PGA, Xanthan). While for  $\Psi_m = -1$  kPa all fluids showed similar values for the loss factor, a treatment-dependent effect can be observed with  $\Psi_m = -3$  kPa and  $\Psi_m = -6$  kPa. Here, a shift to larger values of the loss factor over the complete

deformation range can be observed with the addition of Xanthan. This can be caused by lowered soil stability, due to increased water contents [**Figure 4** and **Table 2** ( $\theta_{\text{before}}$  vs.  $\theta_{\text{PGA}}$  or  $\theta_{\text{XAN}}$ ), (Riggert et al., 2017)] or by the occurrence of positive water pressures (Fazekas and Horn, 2005) due to an increased viscosity of the soil solution (**Figure 2**). Remarkably are the curves for the driest matric potential ( $\Psi_m = -30$  kPa): All flow curves showed a local peak for the loss factor (between 0.1 and 1% deformation), followed by a decrease of the loss factor for deformations around 10%. This decrease is less pronounced for samples saturated with water and most pronounced for samples saturated with PGA. For PGA an absolute minimum for the loss factor can be found. Furthermore, the occurrence of this minimum is achieved with a less pronounced deformation if water was used for saturation compared to PGA or Xanthan. Baumgarten et al. (2013) stated, that the curve's progression is influenced by many soil properties like soil texture, clay mineralogy, particle shape, organic matter compounds, (micro)- aggregate stability and other physicochemical properties. We found out that water

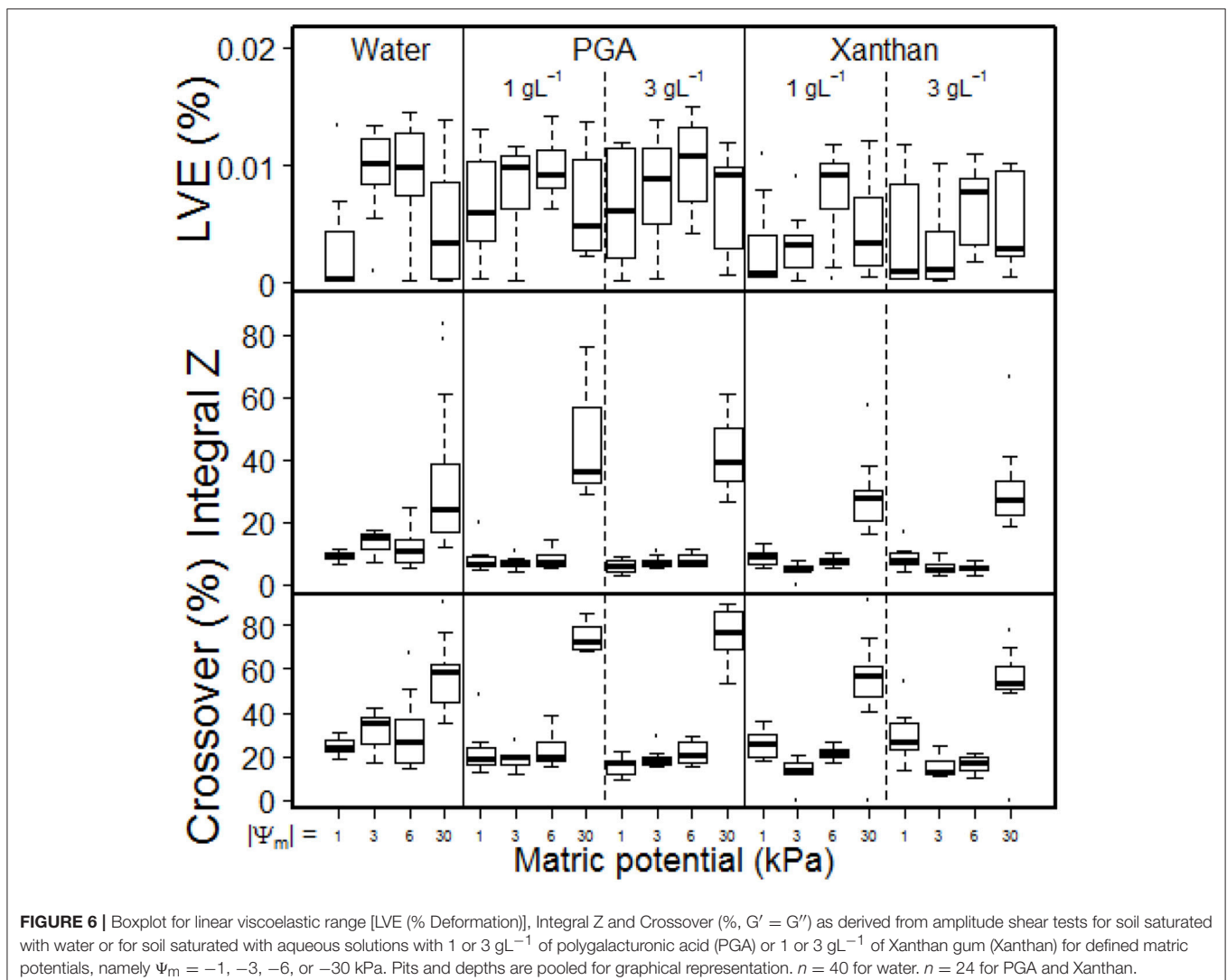


**FIGURE 6** | Boxplot for linear viscoelastic range [LVE (% Deformation)], Integral Z and Crossover (%  $G' = G''$ ) as derived from amplitude shear tests for soil saturated with water or for soil saturated with aqueous solutions with 1 or 3 gL<sup>-1</sup> of polygalacturonic acid (PGA) or 1 or 3 gL<sup>-1</sup> of Xanthan gum (Xanthan) for defined matric potentials, namely  $\Psi_m = -1, -3, -6,$  or  $-30$  kPa. Pits and depths are pooled for graphical representation.  $n = 40$  for water.  $n = 24$  for PGA and Xanthan.

content is the most important parameter on the progression of the curve as it has indeed an influence on (micro)- aggregate stability. It is mandatory, to measure the water content, as a standard parameter, and thus, most appropriate as an input factor to describe the flow behavior of soils. In this study it was found to influence the deformation behavior significantly, while SOC, texture, pH and eC did not. Curves with a locale maximum in loss factors can be found with other soils, for example for several Andisols from Chile (Baumgarten et al., 2013), for salic tidalic fluvisols or fluvi-calcic gleysols (Baumgarten et al., 2012) but until now, a massive decrease like that one shown in **Figure 3** ( $\Psi_m = -30$  kPa) has never been observed but indicates soil stabilization processes caused by deformation: Aggregates disrupt, even if the deformation is mostly elastic (loss factor  $<1$ ). Polyvalent cations (especially  $\text{Ca}^{2+}$ , Santos et al., 1997) are released from the aggregate's interior, agglomerating negatively charged primary clay particles to each other, or leading to the formation of clay-organic associations with negatively charged organic anions like Xanthan or PGA. The fact that  $\text{Mg}^{2+}$  shows no cooperativity between single PGA chains while  $\text{Ca}^{2+}$  leads to the formation of PGA-PGA associations (Malovikova et al., 1994) supports this hypothesis, since the ratio  $\text{Ca}^{2+}$  to  $\text{Mg}^{2+}$  increases from aggregate's exteriors to aggregate's interiors (Santos et al., 1997). Another proof is that this behavior is only found with low degrees in water saturation, because otherwise the amount of released cations might be diluted in the soil solution. The

shift in deformation (%) where the local minimum occurred may be caused by a less intense aggregate disruption with low deformations due to the aggregate's stabilizing effect of PGA and Xanthan. The statistical analysis proved both, the dependency of the loss factor on differing shear rates [expressed in differing deformation-intensities (%)] and the stabilization of soil with its deformation.

## Results and Discussion (Single Point Evaluation)

The statistical results of the single point evaluation (SPE) delivered regression functions for each measurement point (MP, 1–30) which had been applied in the course of the amplitude sweep test. It was used to evaluate the loss- and storage-modulus, the loss factor and the shear stress. The normal force influences significantly storage- and loss-moduli but had no impact on loss factors or shear stresses. The impact of the normal forces was tenfold more pronounced for storage- than for loss moduli (data not shown). All parameters were significantly influenced by interaction effects for the depths and the MP (data not shown). Depth dependent regression parameters for storage moduli are shown in **Figure 7**. The concentration of PGA significantly influenced the storage module up to MP 14 (T0, 0.45–0.55 m) or MP 13 (T1, 0.55–0.65 m), resulting in increasing storage moduli with increasing concentrations. Here, a significant influence for the concentration of Xan was not found. With PGA, the matrix

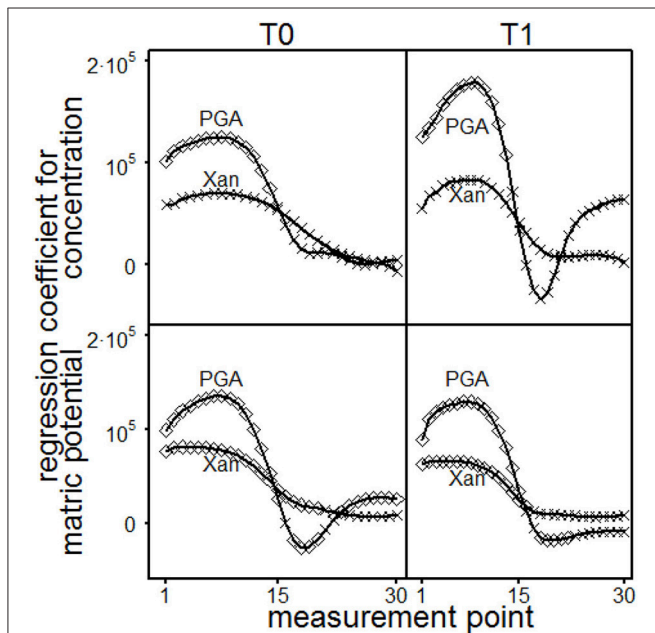


**FIGURE 7** | Results of the single point evaluation for soil material excavated from T0 (0.45 to 0.55 m, left-hand side) or T1 (0.55 to 0.65 m, right-hand side) and saturated with Xanthan gum (Xan) or polygalacturonic acid (PGA): Regression coefficients for storage modulus. Concentration effect: regression coefficients for each measurement point and depth (upper row). Effect of matric potential: regression coefficients for each measurement point and depth (lower row).  $\diamond$  marks a significant influence of the regression coefficient ( $p \leq 0.05$ ) on storage modulus, while  $\times$  represent  $p > 0.05$ .

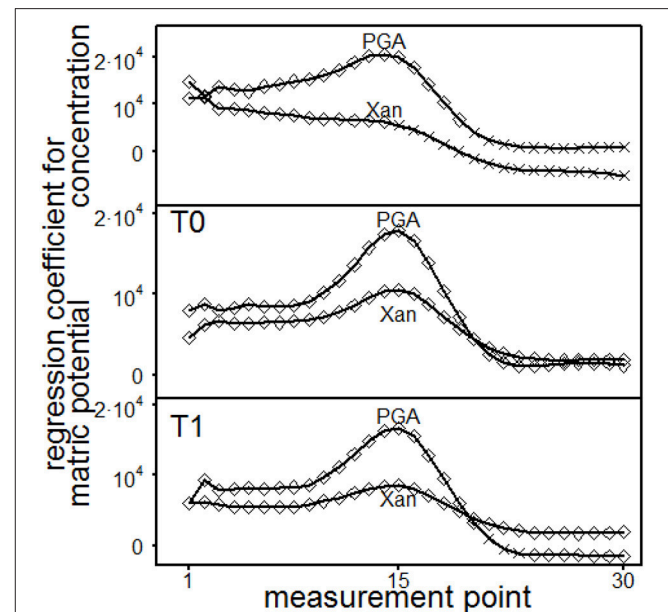


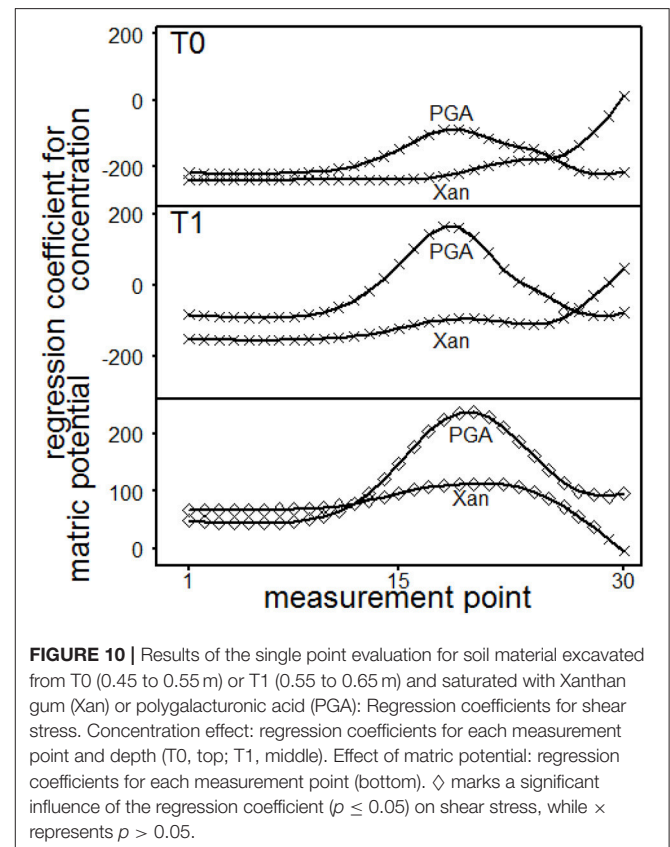
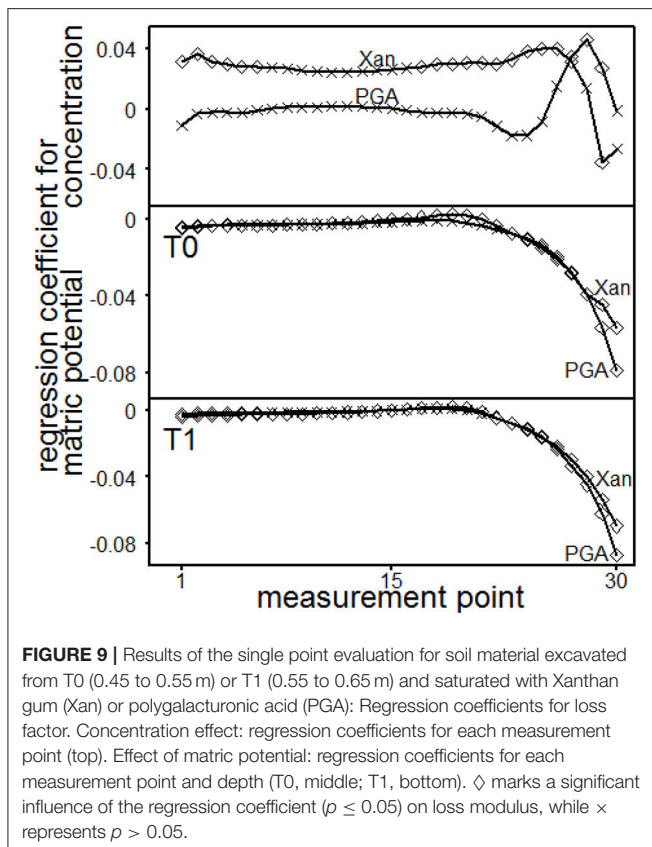
**FIGURE 8** | Results of the single point evaluation for soil material excavated from T0 (0.45 to 0.55 m) or T1 (0.55 to 0.65 m) and saturated with Xanthan gum (Xan) or polygalacturonic acid (PGA): Regression coefficients for loss modulus. Concentration effect: regression coefficients for each measurement point and depth (top). Effect of matric potential: regression coefficients for each measurement point and depth (T0, middle; T1, bottom).  $\diamond$  marks a significant influence of the regression coefficient ( $p \leq 0.05$ ) on loss modulus, while  $\times$  represents  $p > 0.05$ .

potential ( $|\Psi_m|$ ) increased the storage moduli at low ( $MP < 17$ ) and high ( $MP > 21$ ) deformation rates but decreased the storage moduli at intermediate deformation rates for T0 (due to negative regression coefficients). The increasing effect at high deformation rates was not found with T1. The storage moduli significantly increased with increasing matric potential for Xanthan at low deformation rates (up to MP 21 for T0 or up to MP 17 for T1). The concentration effect of the loss-moduli (**Figure 8**) was not depth-dependent but reflects a significant increase in loss moduli with increasing concentrations for Xanthan ( $MP < 15$ ) and PGA ( $MP < 20$ ). The effect of matric-potential significantly increased the loss moduli for Xanthan saturated samples in both depths over the complete deformation range. A significantly increasing effect was also found for PGA ( $MP 1-30$ ) but T1 showed a more differentiated pattern: Here, increases in  $|\Psi_m|$  (=absolute values) resulted in significantly increased values up to MP 21, but significantly decreased values for  $MP > 24$ . The loss factor for PGA increased independently of the depths with increasing concentration at high deformation rates ( $MP 27-28$ ) or for  $MP 1-27$  for Xanthan but decreased for  $MP 29$  (**Figure 9**). Increasing matric potentials resulted in a reduced loss factor in both depths and for both fluids at low deformation rates but the loss factor increased with increasing Xanthan concentrations ( $MP 17-21$  for T0 or  $MP 19-21$  for T1). These results support the theory of (I) soil homogenization in the course of the deformation, and (II) increasing soil stability due to the

establishment of PGA-PGA associations caused by the release of  $Ca^{2+}$  as a consequence of soil homogenization. This is reflected in the absence of a (significant) concentration effect for PGA at low deformation rates but a positive influence at high deformation rates, which was not found for Xanthan.

The shear stress was depth-dependent influenced by the concentration, whereas shear stress increased with increasing Xanthan concentrations, a peak was found with PGA for intermediate deformation rates (**Figure 10**). Increasing matric potential resulted in significantly increased shear stresses for Xan ( $MP 1-28$ ) or PGA ( $1-30$ ). The effect was more pronounced for Xanthan at low deformation rates ( $MP \leq 12$ ) and more pronounced for PGA at higher deformation rates. These results are contradictory to Mohr-Coulombs failure criterion because of the missing influence of the normal force and point out the dependency of shear stresses on deformation rates and furthermore, underline differing impacts of different biological model substances or in general of SOC on soil stability and on the flow behavior of soils.

The presented results underline that plant root growth processes depend not only on physical soil properties (surely driven by a biological process) because these parameters are chemically altered by biological processes with consequences for plant root growth. However, the results point out, that the definition of thresholds (e.g., penetration resistance) for plant-root growth are not appropriate because barriers of plant root



growth can be encountered by naturally altered shear rates, due to slower root growth or by altered water regimes, due to concentration effects of organic compounds exuded at the root's tip resulting in altered shear resistances and altered rheological properties like storage-, loss-moduli and loss factors. These results point out again the complexity of processes occurring in the rhizosphere, in which not only chemicals [like humic acids (Asli and Neumann, 2010), or inorganic salts (Holthusen et al., 2012)] influence e.g., the hydraulic conductivity and thus the plants development. Additionally indirect influences induced by plants or microorganisms occur like an altered root growth due to altered soil stability caused by altered physico-chemical properties like viscosity or surface tension.

## CONCLUSION

All hypotheses were supported by the data, shedding a new light on soil stability and therewith on plant root growth processes in the rhizosphere. The results underline the biological alteration of physical properties, e.g., in the vicinity of biological hot spots like root or earthworm channels or particulate organic matter.

## REFERENCES

- Akaike, H. (1973). "Information theory and an extension of the maximum likelihood principle," in *Proceedings of the Second International Symposium on Information Theory*, eds B. N. Petrov and F. Csaki (Budapest: Akademiai Kiado), 267–281.
- Asli, S., and Neumann, P. M. (2010). Rhizosphere humic acid interacts with root cell walls to reduce hydraulic conductivity and plant development. *Plant Soil* (2010) 336, 313–322. doi: 10.1007/s11104-010-0483-2
- Banfield, C. C., Dippold, M. A., Pausch, J., Hoang, D. T. T., and Kuzyakov, Y. (2017). Biopore history determines the microbial community composition in subsoil hotspots. *Biol. Fertil. Soils* 9:54. doi: 10.1007/s00374-017-1201-5
- Baumgarten, W., Dörner, J., and Horn, R. (2013). Microstructural development in volcanic ash soils from South Chile. *Soil Till Res.* 129, 48–60. doi: 10.1016/j.still.2013.01.007
- Baumgarten, W., Neugebauer, T., Fuchs, E., and Horn, R. (2012). Structural stability of Marshland soils of the riparian zone of the Tidal Elbe River. *Soil Till* 125, 80–88. doi: 10.1016/j.still.2012.06.002
- Bengough, A., and Mullins, C. (1990). Mechanical impedance to root growth: a review of experimental techniques and root growth responses. *Eur. J. Soil Sci.* 41, 341–358. doi: 10.1111/j.1365-2389.1990.tb00070.x
- Carvalhais, L. C., Dennis, P. G., Fedoseyenko, D., Hajirezaei, M.-R., Borriss, R., and von Witrén, N. (2011). Root exudation of sugars, amino acids, and organic acids by maize as affected by nitrogen, phosphorus, potassium, and iron deficiency. *J. Plant Nutr. Soil Sci.* 2010, 1–9. doi: 10.1002/jpln.201000085
- Chang, I., Im, J., Prasadhi, A. K., and Cho, G.-C. (2015). Effects of xanthan gum biopolymer on soil strengthening. *Constr. Building Mat.* 74, 65–72. doi: 10.1016/j.conbuildmat.2014.10.026
- Chenu, C., Le Bissonnais, Y., and Arrouays, D. (2000). Organic matter influence on clay wettability and soil aggregate stability. *Soil Sci. Soc. Am. J.* 64, 1479–1486. doi: 10.2136/sssaj2000.6441479x
- Cochran, W. G. (1957). Analysis of covariance-Its nature and uses. *Biometrics* 13, 261–281. doi: 10.2307/2527916
- Czarnes, S., Hallett, P. D., Bengough, A. G., and Young, I. M. (2000). Root- and microbial-derived mucilages affect soil structure and water transport. *Eur. J. Soil Sci.* 51, 435–443. doi: 10.1046/j.1365-2389.2000.0327.x
- Fazekas, O., and Horn, R. (2005). Zusammenhang zwischen hydraulischer und mechanischer bodenstabilität in Abhängigkeit von der Belastungsdauer. *J. Plant Nutr. Soil Sci.* 168, 60–67. doi: 10.1002/jpln.200421381
- Gessa, C., and Deiana, S. (1992). Ca-polygalacturonate as a model for a soil-root interface. II. Fibrillar structure comparison with natural root mucilage. *Plant Soil* 140, 1–13. doi: 10.1007/BF00012801
- Gessa, C., Deiana, S., Premoli, A., and Ciurli, A. (1997). Redox activity of caffeic acid towards iron (III) complexed in a polygalacturonate network. *Plant Soil* 190, 289–299. doi: 10.1023/A:1004295719046
- Grimal, J. Y., Frossard, E., and Morel, J. L. (2001). Maize root mucilage decreases adsorption of phosphate on goethite. *Biol. Fertil. Soils* 33, 226–230. doi: 10.1007/s003740000312
- Hallett, P. D., Gordon, D. C., and Bengough, A. G. (2003). Plant influence on rhizosphere hydraulic properties: direct measurements using a miniaturized infiltrometer. *N. Pythol.* 157, 597–603. doi: 10.1046/j.1469-8137.2003.00690.x
- Hallett, P. D., and Young, I. M. (1999). Changes to water repellence of soil aggregates caused by substrate-induced microbial activity. *Eur. J. Soil Sci.* 50, 35–40. doi: 10.1046/j.1365-2389.1999.00214.x
- Hoang, D. T. T., Pausch, J., Razavi, B. S., Kuzyakova, I., Banfield, C. C., and Kuzyakov, Y. (2016). Hotspots of microbial activity induced by earthworm burrows, old root channels, and their combination in subsoil. *Biol. Fertil. Soils* 52, 1105–1119. doi: 10.1007/s00374-016-1148-y
- Holthusen, D., Haas, C., Peth, S., and Horn, R. (2012). Are standard values the best choice? a critical statement on rheological soil fluid properties viscosity and surface tension. *Soil Till. Res.* 125, 61–71. doi: 10.1016/j.still.2012.07.007
- Holthusen, D., Pétile, P., Reichert, J. M., and Horn, R. (2017). Controlled vertical stress in a modified amplitude sweep test (rheometry) for the determination of soil microstructure stability under transient stresses. *Geoderma* 295, 129–141. doi: 10.1016/j.geoderma.2017.01.034
- Holthusen, D., Peth, S., and Horn, R. (2010). Impact of potassium concentration and matric potential on soil stability derived from rheological parameters. *Soil Till. Res.* 111, 75–85. doi: 10.1016/j.still.2010.08.002
- IUSS Working Group WRB (2006). *World Reference Base for Soil Resources*, World Soil Resources Reports No 103 (Rome).
- Jones, D. L., Nguyen, C., and Finlay, R. D. (2009). Carbon flow in the rhizosphere: carbon trading at the soil-root interface. *Plant Soil* 321:5–33. doi: 10.1007/s11104-009-9925-0

## AUTHOR CONTRIBUTIONS

All authors listed have made a substantial, direct and intellectual contribution to the work, and approved it for publication.

## ACKNOWLEDGMENTS

This study was funded by the German Research Foundation (DFG), Bonn, under grants PAK 888. We thank MSc. Phillip Lange (LANUV NRW, Leibnizstr. 10, 45659 Recklinghausen) for the determination of flow properties of soil samples saturated with water. Many thanks to the reviewers for their helpful comments.

- Kautz, T., Amelung, W., Ewert, F., Gaiser, T., Horn, R., Jahn, R., et al. (2012). Nutrient acquisition from arable subsoils in temperate climates: a review. *Soil Biol. Biochem.* 57, 1003–1022. doi: 10.1016/j.soilbio.2012.09.014
- Kautz, T., Lüsebrink, M., Pätzold, S., Vetterlein, D., Pude, R., Athmann, M., et al. (2014). Contribution of anecic earthworms to biopore formation during cultivation of perennial ley crops. *Pedobiologia* 57, 47–52. doi: 10.1016/j.pedobi.2013.09.008
- Laird, N. M., and Ware, J. H. (1982). Random-effects models for longitudinal data. *Biometrics* 38, 963–974. doi: 10.2307/2529876
- Malovikova, A., Rinaudo, M., and Milas, M. (1994). Comparative interactions of magnesium and calcium counterions with polygalacturonic acid. *Biopolymers* 34, 1059–1064. doi: 10.1002/bip.360340809
- Manunza, B., Deiana, S., Pintore, M., and Gessa, C. (1997). A molecular dynamics investigation on the occurrence of helices in polygalacturonic acid. *J. Mol. Struct.* 419, 169–172. doi: 10.1016/S0166-1280(97)00247-9
- Markgraf, W., and Horn, R. (2006). Rheological-stiffness analysis of K<sup>+</sup>-treated and CaCO<sub>3</sub>-rich soils. *J. Plant Nutr. Soil Sci.* 169, 411–419. doi: 10.1002/jpln.200521934
- Markgraf, W., Horn, R., and Peth, S. (2006). An approach to rheometry in soil mechanics - structural changes in bentonite, clayey and silty soils. *Soil Till. Res.* 91, 1–14. doi: 10.1016/j.still.2006.01.007
- Markgraf, W., Moreno, F., and Horn, R. (2012). Quantification of microstructural changes in salorthidic fluvaquents using rheological and particle charge techniques. *Vadose Zone J.* 11, 1–11. doi: 10.2136/vzj2011.0061
- Mezger, T. (2014). *The Rheology Handbook: for Users of Rotational and Oscillatory Rheometers*. Hannover: Vincentz Network
- Mohamed, A., Trickett, K., Chin, S. Y., Cummings, S., Sagisaka, M., Hudson, L., et al. (2010). Universal surfactant for water, oils, and CO<sub>2</sub>. *Langmuir* 26, 13861–13866. doi: 10.1021/la102303q
- Morel, J., Andreux, F., Habib, L., and Guckert, A. (1987). Comparison of the adsorption of maize root mucilage and polygalacturonic acid on montmorillonite homoionic to divalent lead and cadmium. *Biol. Ferti. soils* 5, 13–17. doi: 10.1007/BF00264339
- Morel, J. L., Mench, M., and Guckert, A. (1986). Measurement of Pb<sup>2+</sup>, Cu<sup>2+</sup> and Cd<sup>2+</sup> binding with mucilage exudates from maize (*Zea mays* L) Roots. *Biol. Fertil. Soils* 2, 29–34. doi: 10.1007/BF00638958
- Nakagawa, S., and Schielzeth, H. (2013). A general and simple method for obtaining R<sup>2</sup> from generalized linear mixed-effects models. *Methods Ecol. Evol.* 4, 133–142. doi: 10.1111/J.2041-210x.2012.00261.X
- Pettitt, D. J., Wayne, J. E. B., Renner Nantz, J., and Shoemaker, C. F. (1995). Rheological Properties of Solutions and Emulsions Stabilized with Xanthan Gum and Propylene glycol Alginate. *J. Food. Sci. Vol.* 60, 528–531. doi: 10.1111/j.1365-2621.1995.tb09819.x
- R Development Core Team (2017). *R: A Language and Environment for Statistical Computing*. R Foundation for Statistical Computing, Vienna, Austria. Available online at: <http://www.R-project.org>
- Read, D. B., and Gregory, P. J. (1997). Surface tension and viscosity of axenic maize and lupin root mucilages. *N. Phytol.* 137, 623–628. doi: 10.1046/j.1469-8137.1997.00859.x
- Riggert, R., Fleige, H., Kietz, B., Gaertig, T., and Horn, R. (2017). Dynamic stress measurements and the impact of timber harvesting on physical soil properties *Aust. Forestry* 80, 255–263. doi: 10.1080/00049158.2017.1347981
- Sakamoto, Y., Ishiguro, M., and Kitagawa, G. (1986). *Akaike Information Criterion Statistics*. Dordrecht: D. Reidel Publishing Company.
- Santos, D., Smucker, A. J. M., Murphy, S. L. S., Taubner, H., and Horn, R. (1997). Uniform separation of concentric surface layers from soil aggregates. *Soil Sci. Soc. Am. J.* 61, 720–724. doi: 10.2136/sssaj1997.03615995006100030003x
- Six, J., Bossuyt, H., Degryze, S., and Deneff, K. (2004). A history of research on the link between (micro)aggregates, soil biota, and soil organic matter dynamics. *Soil Till. Res.* 79, 7–31. doi: 10.1016/j.still.2004.03.008
- Stoddart, R. W., Spires, I. P. C., and Tipton, K. F. (1969). Solution properties of polygalacturonic acid. *Biochem. J.* 114, 863–870. doi: 10.1042/bj1140863
- Tisdall, J. M., and Oades, J. M. (1979). Stabilization of soil aggregates by the root systems of ryegrass. *Soil Res.* 17, 429–441. doi: 10.1071/SR9790429
- Traoré, O. V., Groleau-Renaud, S., Planteureux, A., Tubeileh, and Boeuf-Tremblay, V. (2000). Effect of root mucilage and modelled root exudates on soil structure. *Eur. J. Soil Sci.* 51, 575–581. doi: 10.1046/j.1365-2389.2000.00348.x
- Uteau, D., Hafner, S., Pagenkemper, S. K., Peth, S., Wiesenberger, G. L. B., Kuzyakov, Y., et al. (2015). Oxygen and redox potential gradients in the rhizosphere of alfalfa grown on a loamy soil. *J. Plant Nutr. Soil Sci.* 178, 278–287. doi: 10.1002/jpln.201300624
- Verbeke, G., and Molenberghs, G. (2000). *Linear Mixed Models for Longitudinal Data*. New York, NY: Springer.
- Zhang, B., Hallett, P. D., and Zhang, G. (2008). Increase in the fracture toughness and bond energy of clay by a root exudate. *Eur. J. Soil Sci.* 59, 855–862. doi: 10.1111/j.1365-2389.2008.01045.x

**Conflict of Interest Statement:** The authors declare that the research was conducted in the absence of any commercial or financial relationships that could be construed as a potential conflict of interest.

Copyright © 2018 Haas, Holthusen and Horn. This is an open-access article distributed under the terms of the Creative Commons Attribution License (CC BY). The use, distribution or reproduction in other forums is permitted, provided the original author(s) and the copyright owner(s) are credited and that the original publication in this journal is cited, in accordance with accepted academic practice. No use, distribution or reproduction is permitted which does not comply with these terms.